Highly efficient and ultrabroadband hybrid Silicon-Lithium Niobate grating coupler

Quan Shi [1+]
School of electronic science and engineering
Southeast university
Nanjing, China
quan_shi@seu.edu.cn

Dongli Dai[1,2+]
School of electronic science and engineering
Southeast university
Nanjing, China
dongli.dai@seu.edu.cn

Xinyao Wu
School of electronic science and engineering
Southeast university
Nanjing, China
xy_wu@seu.edu.cn

Haoyu Luo
School of electronic science and engineering
Southeast university
Nanjing, China
hyluo@seu.edu.cn

Kaiyi Li
School of electronic science and engineering
Southeast university
Nanjing, China
kyli@seu.edu.cn

Tong Lin*
School of electronic science and engineering
Southeast university
Nanjing, China
lintong@seu.edu.cn

+These authors contributed equally to this work

***Abstract*—We propose and design a highly efficient and ultrabroadband grating coupler based on the hybrid Silicon and Lithium Niobate platform. By using a triple layer structure and a bottom metal reflector, simulation results demonstrate that the minimal insertion loss is about -0.15dB and the 1-dB optical bandwidth is up to 135 nm. Such a broadband and highly-efficient grating coupler is suitable for various thin film Lithium Niobate devices.**

Keywords—Integrated optics, diffraction gratings, chirped grating coupler, thin-film Lithium Niobate

I. INTRODUCTION

Lithium Niobate (LN) has emerged as a significant material due to its promising optical nonlinear properties, exceptionally low optical absorption loss across a wide spectral range (400nm~5um), and robust physicochemical stability in the past few decades[1]. These properties enable bulk LN to be successfully applied in commercial applications, such as wide-band electro-optic and acousto-optic modulators[2], [3], frequency conversion[4], etc. Recently, thin film LN (TFLN) on the insulator become available in a wafer scale through bonding and ion dicing techniques[5], facilitating the strongly confined waveguides due to the large refractive index contrast to the silicon dioxide[6]. Therefore, the ultracompact footprints of TFLN devices compared to the bulk LN counterparts significantly enhance the nonlinear efficiency, increase the bandwidth, and reduce the power consumption. TFLN, the novel platform, is gaining increasing prominence for its utility in versatile photonic integrated circuits (PICs)[7].

To efficiently couple the light among the TFLN devices and optical fibers, a grating coupler (GC) is one key candidate, allowing for the dense integration and wafer-scale testing capability. Currently, three main types of TFLN GCs prevail. The first one uses argon plasma etching to form all the waveguide structures and fine grating teeth. Usually, the dry-etched TFLN sidewall angle is not vertical and hard to control[8], resulting in poor reproducibility, low yield, and high manufacturing cost. The second GC design utilizes Bound states in the continuum (BIC)[9] to avoid LN etching. These BIC GCs can only work in the TM mode due to the BIC mechanism, severely limiting the device versatility. The third GC design is based on a hybrid waveguide formed between another material (Si3N4, α-Si, etc.) and LN. The waveguide is defined by only etching the upper layer to avoid LN etch. However, only part of the optical mode resides in the LN, resulting in poor electro-optic effects and small electro-optic bandwidths [7],[10] ,[11].

In this paper, we propose a hybrid α-Si-LN GC with an ultralow coupling loss and ultrabroad bandwidth. Our design only etches non-critical LN slab waveguide, where the angled sidewalls do not have impacts on the GC performance. The grating teeth are defined in the deposited α-Si layer, where the mature Si etching process guarantees the reproducibility. In addition, the Bloch mode in the GC is gradually converted into the LN waveguide mode, employing the full potential of the TFLN platform. Our design also shows a high level of process tolerance.

II. PRINCIPLE

A. The theory of grating coupler

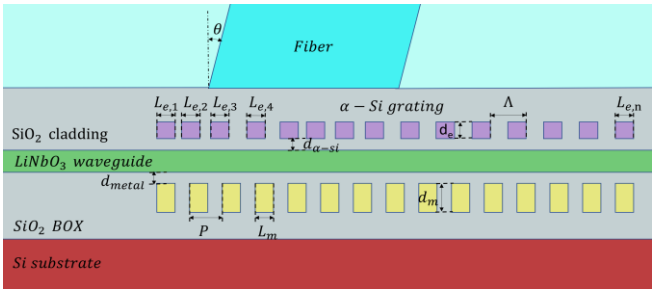

Fig. 1. The structure of our grating coupler.

Fig. 1 shows our proposed structure of the hybrid grating coupler with a patterned bottom metal reflector. The grating teeth are formed within the amorphous silicon (α-Si) layer, rather than the LN layer, which can be precisely controlled using the reliable Si-based fabrication processes. The spacing between the LN layer and the α-Si layer is $d_{\alpha-si}$. The LN layer is positioned above a buried silicon dioxide layer on a silicon substrate, and is covered by an oxide cladding layer. The LN layer is 600 nm thick, enabling both strong nonlinear interaction and dispersion engineering[10]. A gold reflector, positioned below the LN layer at a distance of d_{metal}, recycles leaked light and enhances overall coupling efficiency.

According to the first-order Bragg condition, the period of the grating (Λ) is given by (1):

$$\Lambda = \frac{\lambda_c}{(N_{eff} - \sin\theta_c)} \quad (1)$$

where λ_c is the incident wavelength, θ_c is the diffraction angle, and N_{eff} is the effective refractive index of the grating teeth. As a key parameter, the effective index N_{eff} depends on the duty cycle and two material indices, and is given by (2):

$$N_{eff} = F_n \cdot N_O + (1 - F_n) \cdot N_E \quad (2)$$

where F_n is the grating duty cycle (n=1,2,…,n), N_O and N_E are the refractive indices of the cladding silicon dioxide and the amorphous silicon respectively. We apply a linear apodization to the α-Si grating for a better mode overlap between the grating and the single-mode fiber[11]. Therefore, the length of each α-Si grating tooth is different and denoted as $L_{e,n}$ (n=1,2,…,n). Here the grating duty cycle F_n for each grating tooth is defined as (3):

$$F_n = F - R \cdot (n-1), n \in \mathbb{N}_+ \quad (3)$$

where F is the initial duty cycle of the first radiation unit, R is the step size of the linear variation, and n is the n_{th} coupling unit in the grating.

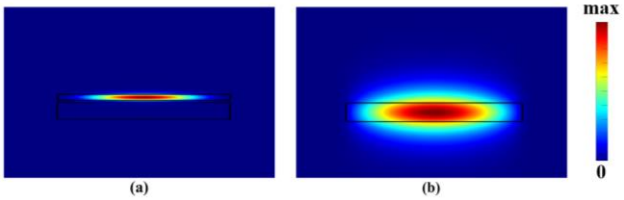

Fig. 2. (a) Mode field distribution in the hybrid α-Si-LN slab waveguide (width of 20 μm, spacing of 0.09 μm, α-Si height of 0.22 μm, LN height of 0.6 μm). (b) Mode field distribution for the slab LN waveguide only (width of 20 μm, height of 0.6 μm).

It increases linearly from the access waveguide, improving the optical impedance matching and reducing the reflection.

Fig.2 shows the mode distributions for the hybrid α-Si-LN slab waveguide and LN slab waveguide respectively. The hybrid bi-layer structure makes the light field reside mostly in the upper layer as shown in Fig.2.(a). In this paper, we choose α-Si as it has a higher refractive index than LN, which is able to pull the light out of the LN waveguide more efficiently. In this way, the diffracted light can be engineered there without fabricating critical grating structures in the LN layer. In contrast, the conventional LN slab waveguide need to be etched to from a grating coupler as shown in Fig.2.(b), which is hard to control.

The α-Si grating coupler consists of an apodised grating region and a uniform Bragg grating region. The parameters of the apodised Bragg grating region are designed first, followed by the uniform Bragg grating part. It is noted that the duty cycle of the uniform grating equals that of the last cell of the apodised grating tooth. Last, the bottom metal reflector is induced to improve the directionality of the reflected light and further increase the coupling efficiency. Different from the upper α-Si grating, this metal layer is designed to be a uniform grating.

III. Simulation and Results

We design the hybrid α-Si-LN grating coupler using the FDTD method and optimize it with the particle swarm optimization algorithm (PSO). The following parameters are modified including Λ, d_e, N, F, P, F_m, d_{metal}, $d_{\alpha-si}$, x, θ, R, F_1, F_2, F_3 , and F_4 where x and θ denote the position and angle of the optical fiber. The first four teeth (F_1, F_2, F_3 , F_4) of the α-Si grating are modified independently in order to match the fiber's Gaussian-like mode profile. The final optimized parameters of the proposed grating are shown in Table I.

TABLE I. OPTIMIZED STRUCTURAL PARAMETERS OF THE PROPOSED GC

Parameters	$\boldsymbol{\Lambda(\mu m)}$	$\boldsymbol{d_e(\mu m)}$	$\boldsymbol{N}$
Values	0.88	0.22	9
Parameters	$\boldsymbol{F}$	$\boldsymbol{P(\mu m)}$	$\boldsymbol{F_m}$
Values	0.40	0.90	0.40
Parameters	$\boldsymbol{d_{metal}(\mu m)}$	$\boldsymbol{d_{\alpha-si}(\mu m)}$	$\boldsymbol{x(\mu m)}$
Values	0.17	0.09	-2.71
Parameters	$\boldsymbol{\theta}$	$\boldsymbol{R}$	$\boldsymbol{L_{e,1}(\mu m)}$
Values	8.5°	0.015	0.49
Parameters	$\boldsymbol{L_{e,2}(\mu m)}$	$\boldsymbol{L_{e,3}(\mu m)}$	$\boldsymbol{L_{e,4}(\mu m)}$
Values	0.44	0.40	0.37

Fig. 3(a) shows the coupling efficiency in the wavelength range of 1450-1650 nm with the optimized parameters. The insertion loss is as low as -0.15 dB (96.5%) at 1548 nm wavelength and changes slowly to - 4.24(-4.25) dB at 1650 (1460) nm. For the entire C-band, our grating coupler's insertion loss ranges from -0.15 dB to -0.23 dB, which is beneficial in metro, long-haul, ultra-long-haul, and submarine fiber optic systems. It has a 1-dB-bandwidth of 135 nm (1497-1632 nm) and a 3-dB-bandwidth of 185 nm (1470-1655 nm). One reason lies that the virtual directional coupler formed by the α-Si/SiO_2/LN layer permits a larger bandwidth[12]. Without the bottom metal grating, the maximum achievable insertion loss is about -2.1 dB as shown in the purple dashed line of Fig. 3.(a). In this case, the loss mainly comes from the downward diffracted light. In contrast, this leakage loss can be reduced down to about -25 dB with the bottom metal reflector as shown in Fig. 3.(b). It proves the functionality of

the metal layer, which recycles the downward light. Fig. 3.(c) shows the electrical field distribution at the wavelength of 1550 nm where the light enters from the left LN waveguide. Almost all the light diffracts upward at an angle of 8.5°, and readily to be collected by a single mode fiber.

Fig. 3.(c) shows the electrical field distribution at the wavelength of 1550 nm where the light enters from the left LN waveguide. Almost all the light diffracts upward at an angle of 8.5°, and readily to be collected by a single mode fiber.

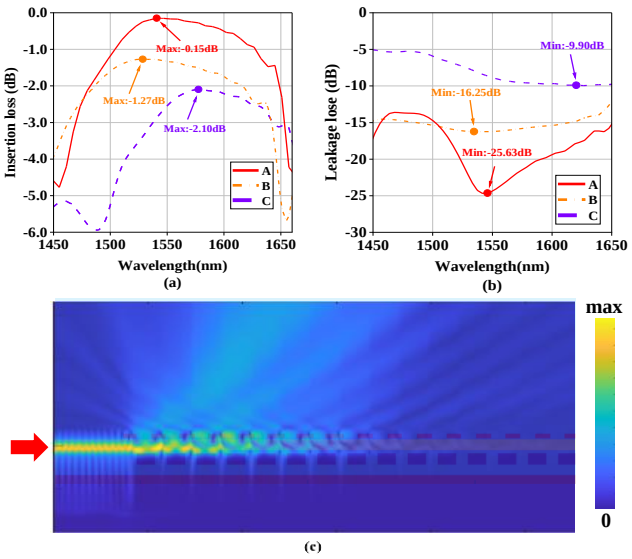

Fig. 3. (a) The transmission spectra of the GC with a metal grating [A], the GC with a conventional metal reflector [B], the hybrid GC alone[C]. (b) The downward leakage loss of the GC with a metal grating [A], the GC with a conventional metal reflector [B], the hybrid GC alone[C]. (c) The light field distribution injected from the waveguide at the wavelength of 1550 nm.

We demonstrate that our design is robust to fabrication imperfections. Four typical structural parameters (F_m, P, R, Λ) are varied around the optimal values and the insertion loss is simulated in each scenario. As shown in Fig.4.(a), the insertion loss decreases within 0.25 dB in the wavelength range from 1540 nm to 1560 nm for F_m is within ±0.10 range of its optimum value. Similarly, when P, R and Λ vary within ±0.10 μm, ±0.010, and ±0.025 μm around their optimal values respectively, the insertion loss decreases within 0.7 dB. The overall sensitivity of the designed grating coupler to fabrication imperfections is low, and the coupling efficiency can still be maintained at a high level.

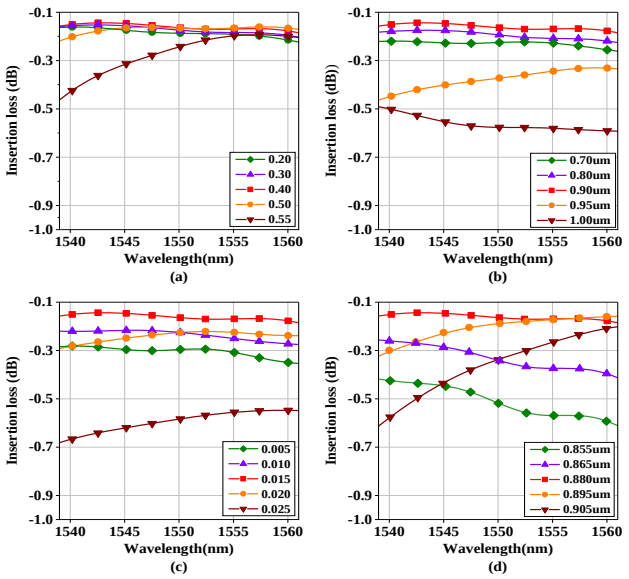

Fig. 4. Comparison of insertion loss when parameters fluctuate around the optimal value: (a) metal reflector layer duty cycle (F_m); (b) metal reflector layer period (P); (c) etched chirped step rate (R); (d) α-silicon grating period (Λ).

TABLE Ⅱ gives a performance comparison of the reported GCs on the LNOI platform recently, among which the lowest insertion loss is around -0.5 dB and the 3-dB bandwidth is about 90 nm respectively. Our proposed design has theoretically the lowest insertion loss and largest bandwidth.

TABLE II. PERFORMANCE COMPARISON OF SOME REPORTED GRATING COUPLERS ON LNOI

Design structure	CE (dB)	Bandwidth (nm)	Theory/ Experiment	Fabrication Process
Bragg GC[13]	-6.2	/	Theory	EBL+EBE
Bragg gratings on TFLN[14]	-8.37	80(-3dB)	Theory	EBL+RIE
GC with a metal bottom reflector[15]	-6.9	/	Theory	EBE+ FIB
Ridge-waveguide LNOI GCs with SWG waveguide [3]	-5.1	90(-3dB)	Theory	EBL+DE
Chirped and apodised GC[8]	-3.3	90(-3dB)	Theory	EBL+ICP-RIE(Ar^+)
Bragg GC with $\alpha - Si$ grating teeth[16]	-3.09	59(-1dB)	Experiment	EBL+ICP+ ICP-CVD +CVD+ICP（HBr）
Chirped Bragg GC[17]	-1.56	67(-3dB)	Theory	/
Chirped GC with Au reflector[18]	-0.52	/	Experiment	EBL+ICT
Our work	-0.22	185(-3dB)	Theory	/

IV. Conclusion

We design a highly efficient and ultrabroadband hybrid a-Si-LN grating coupler with grating metal reflector. The insertion loss is as low as -0.15 dB and the 1-dB bandwidth is up to 135 nm. We also analyze the fabrication tolerances of our design. The simulation results reveal that the insertion loss changes to less than 0.7 dB when the geometry changes up to 300 nm. Our design only etches the non-critical LN slab waveguide, a process that ensures GC reproducibility but may constrain integration during fabrication. The proposed GC will promote the wide use of the emerging LiNbO3 platform and will allow for the utilization of the hybrid advantages of silicon and LiNbO3.

References

[1] Y. Qi and Y. Li, "Integrated lithium niobate photonics," Nanophotonics, vol. 9, no. 6, pp. 1287–1320, 2020, doi: doi:10.1515/nanoph-2020-0013.

[2] L. Cai et al., "Acousto-optical modulation of thin film lithium niobate waveguide devices," Photon. Res., vol. 7, no. 9, pp. 1003–1013, Sep. 2019, doi: 10.1364/PRJ.7.001003.

[3] S. Yang, Y. Li, J. Xu, L. Wu, X. Quan, and X. Cheng, Sub-wavelength Gratings Assisted Ridge Waveguide Surface Couplers on Lithium Niobate Thin Film. 2021. doi: 10.1364/OFC.2021.Th1A.23.

[4] J. Yu, Z. Jia, L. Yi, Y. Su, G.-K. Chang, and T. Wang, "Optical millimeter-wave generation or up-conversion using external modulators," IEEE Photonics Technology Letters, vol. 18, no. 1, pp. 265–267, 2006, doi: 10.1109/LPT.2005.862006.

[5] R. Ge, J. Wu, X. Liu, Y. Chen, and X. Chen, "Recent progress in thin-film lithium niobate photonic crystal \[Invited\]," Chin. Opt. Lett., vol. 22, no. 3, p. 033602, Mar. 2024.

[6] L. Cheng, S. Mao, Z. Li, Y. Han, and H. Y. Fu, "Grating Couplers on Silicon Photonics: Design Principles, Emerging Trends and Practical Issues," Micromachines, vol. 11, no. 7, 2020, doi: 10.3390/mi11070666.

[7] D. Zhu et al., "Integrated photonics on thin-film lithium niobate," Adv. Opt. Photon., vol. 13, no. 2, pp. 242–352, Jun. 2021, doi: 10.1364/AOP.411024.

[8] X. He, D. Sun, J. Chen, and Y. Shi, "Inverse Designed Grating Coupler With Low Loss and High Bandwidth on LNOI Platform," IEEE Photonics Journal, vol. 16, no. 1, pp. 1–5, 2024, doi: 10.1109/JPHOT.2024.3351199.

[9] Z. Huang et al., "Highly efficient second harmonic generation of thin film lithium niobate nanograting near bound states in the continuum," Nanotechnology, vol. 32, no. 32, p. 325207, May 2021, doi: 10.1088/1361-6528/abfe23.

[10] C. Wang et al., "Metasurface-assisted phase-matching-free second harmonic generation in lithium niobate waveguides," Nature Communications, vol. 8, no. 1, p. 2098, Dec. 2017, doi: 10.1038/s41467-017-02189-6.

[11] A. Bozzola, L. Carroll, D. Gerace, I. Cristiani, and L. C. Andreani, "Optimising apodized grating couplers in a pure SOI platform to -0.5 dB coupling efficiency.," Optics express, vol. 23 12, pp. 16289–304, 2015.

[12] R. Korček et al., "Low-loss grating coupler based on inter-layer mode interference in a hybrid silicon nitride platform," Opt. Lett., OL, vol. 48, no. 15, pp. 4017–4020, Aug. 2023, doi: 10.1364/OL.495371.

[13] M. Nisar, Z. Xiangjie, an Pan, S. Yuan, and J. Xia, "Grating Coupler for on-chip Lithium Niobate Ridge Waveguide," IEEE Photonics Journal, vol. PP, pp. 1–1, Dec. 2016, doi: 10.1109/JPHOT.2016.2630314.

[14] M. A. Baghban, J. Schollhammer, C. Errando-Herranz, K. B. Gylfason, and K. Gallo, "Bragg gratings in thin-film LiNbO3 waveguides," Opt. Express, vol. 25, no. 26, pp. 32323–32332, Dec. 2017, doi: 10.1364/OE.25.032323.

[15] Z. Chen, R. Peng, Y. Wang, H. Zhu, and H. Hu, "Grating coupler on lithium niobate thin film waveguide with a metal bottom reflector," Opt. Mater. Express, vol. 7, no. 11, pp. 4010–4017, Nov. 2017, doi: 10.1364/OME.7.004010.

[16] J. Jian et al., "High-efficiency hybrid amorphous silicon grating couplers for sub-micron-sized lithium niobate waveguides," Opt. Express, vol. 26, no. 23, pp. 29651–29658, Nov. 2018, doi: 10.1364/OE.26.029651.

[17] M. Liu, B. Xu, G. Meng, J. Du, J. Sun, and J. Wang, "Design and Simulation of Highly Efficient Chirped Blazed Grating Coupler Based on Thin-Film Lithium Niobate," in 2023 Asia Communications and Photonics Conference/2023 International Photonics and Optoelectronics Meetings (ACP/POEM), 2023, pp. 1–3. doi: 10.1109/ACP/POEM59049.2023.10368666.

[18] S. Kang et al., "High-efficiency chirped grating couplers on lithium niobate on insulator," Opt. Lett., vol. 45, no. 24, pp. 6651–6654, Dec. 2020, doi: 10.1364/OL.412902.